Available online at www.sciencedirect.com
SCIENCE DIRECT®
Thermochimica Acta 424 (2004) 149–155
thermochimica acta
www.elsevier.com/locate/tca

Thermal stability and kinetics of ylide-borane complexes

Jonathan M. Stoddard, Kenneth J. Shea*

Department of Chemistry, University of California, Irvine, CA 92612-2025, USA

Received 3 September 2003; received in revised form 21 May 2004; accepted 24 May 2004
Available online 19 July 2004

Abstract

Complexes of dimethylsulfoxonium methylide (**1**) and organoboranes are crystalline for ylide·BH_3 (**2**), ylide·BPh_3 (**3**), ylide·$B(C_6F_5)_3$ (**4**), and ylide·BF_3 (**5**). These complexes undergo exothermic rearrangement by 1,2-migration upon heating to produce homologated organoboranes and dimethylsulfoxide. Non-isothermal kinetic analysis of the differential scanning calorimetry (DSC) data for ylide·BPh_3 (**3**) and ylide·$B(C_6F_5)_3$ (**4**) complexes was applied using the Flynn–Wall–Ozawa and Kissinger methods. The calculated apparent activation energy for the reaction of ylide·BPh_3 (**3**) yielded consistent results between the $A_{1.5}$ model ($E_a = 120\,kJ\,mol^{-1}$, $A = 4.79 \times 10^{13}\,min^{-1}$) and Kissinger method ($E_a = 129\,kJ\,mol^{-1}$, $A = 1.73 \times 10^{17}\,min^{-1}$). The analysis for the reaction of ylide·$B(C_6F_5)_3$ (**4**) gave consistent results between R_2, R_3, and F_1 models with the average parameters, $E_a = 262\,kJ\,mol^{-1}$, $A = 3.33 \times 10^{33}\,min^{-1}$. The Kissinger analysis for the reaction of ylide·$B(C_6F_5)_3$ (**4**) gave Arrhenius activation parameters ($E_a = 171\,kJ\,mol^{-1}$, $A = 7.80 \times 10^{19}\,min^{-1}$) that were higher than for the reaction of ylide·BPh_3 (**3**). The kinetic data revealed that the C_6F_5 electron-deficient group has a higher activation energy for 1,2-migration and a higher entropy of activation for 1,2-migration than the C_6H_5 group. HF/6-31G(d) ab initio calculations agree with the kinetic data.

Keywords: DSC; Non-isothermal; Kissinger kinetics; Homologation

1. Introduction

Trialkylboranes react with the ylide dimethylsulfoxonium methylide (**1**) to produce homologated boranes and dimethylsulfoxide (DMSO) (Scheme 1). In the presence of excess ylide, repetitive homologation results in the formation of polymethylene [1]. The solution kinetics of triethylborane with excess ylide was analyzed to obtain the reaction order and rate of propagation [1]. The rate of initiation (ethyl migration) of alkylboranes has been *assumed* to be *identical* with the rate of propagation (*n*-alkyl migration). The rates of initiation of other organoboranes such as Ph_3B (phenyl migration) and BH_3 (hydride migration) are of interest.

There are two reasons for developing a method to measure the rates of initiation. First, different Lewis acids used for the polyhomologation reaction exhibit significant differences in reactivity of the borane-ylide complex. These differences in reactivity arise due to differences in the activation energy of the group undergoing 1,2-migration. It was thought that a suitable group may be developed that does not undergo 1,2-migration, but allows the other two alkyl groups to undergo 1,2-migration. This is termed a blocking group when polyhomologation occurs selectively along the other alkyl chains. Such a catalyst would allow the synthesis of novel polymethylene architectures and copolymers. Second, the rate of 1,2-phenyl migration from Ph_3B, for example, is directly related to the rate of initiation, k_{in}. In "living" polymerizations, the rate of initiation must be greater than or equal to the rate of propagation, k_{prop}. This criterion, $k_{in} > k_{prop}$, is necessary for the simultaneous start of the polymerization reaction that leads to a narrow molecular weight distribution. However, the rates of initiation cannot be determined by analyzing the kinetics with excess ylide. This report involves the development of a method to measure the rates of initiation directly from the ylide-borane complex.

The initiation of the polyhomologation reaction involves the injection of a small amount of trialkylborane into an excess amount of preheated ylide in toluene. Reaction temperatures from 70 to 80 °C are often used to ensure the solubilization of the developing tris-polymethylene organoborane. Often, an exothermic reaction is observed upon the addition of the initiator, as evidenced by the refluxing

* Corresponding author.
E-mail address: kjshea@uci.edu (K.J. Shea).

0040-6031/$ – see front matter © 2004 Elsevier B.V. All rights reserved.
doi:10.1016/j.tca.2004.05.024

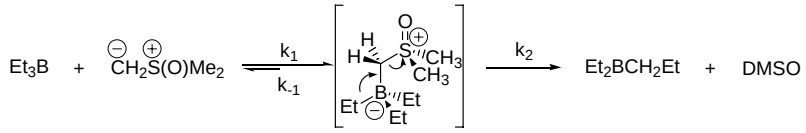

Scheme 1. Sequence of homologation reaction.

solvent, toluene (bp = 110 °C). This exothermicity is likely due to the enthalpic change associated with 1,2-migration.

The synthesis, isolation, and characterization [2] of the complexes between dimethylsulfoxonium methylide (**1**) and BH_3, BPh_3, BF_3, and $B(C_6F_5)_3$ have been previously reported. In solution, ylide·BH_3 (**2**) and ylide·BPh_3 (**3**) undergo spontaneous rearrangement via 1,2-migration at 0 °C, whereas ylide·$B(C_6F_5)_3$ (**4**) and ylide·BF_3 (**5**) are unreactive at room temperature. However, all these complexes can be prepared as crystalline solids that are stable at room temperature. It was thought that the 1,2-rearrangement of these complexes may occur upon heating from either the solid state or the melt to afford homologated reaction products. Differential scanning calorimetry (DSC) was used to obtain kinetic data for the solid-state reaction of complexes **3** and **4**.

The Arrhenius activation parameters for solution-phase reactions are obtained with the Van't Hoff plot method when the order of reaction is known. Reaction rates at various temperatures are used to generate an Arrhenius plot to obtain activation parameters. DSC non-isothermal kinetics differs in that all temperatures are probed during a single heating experiment. However, DSC data must be analyzed by finding the appropriate topochemical model for the reaction [3,4]. The appropriateness of this model can be established graphically, by plotting $\log g(\alpha)\beta$ versus $1/T$, and testing for the generation of linear plots. The variables, α and β refer to the degree of conversion and heating rate (°C min^{-1}), respectively, where $g(\alpha)$ is related to the model of reaction (see below). From these linear plots, one can calculate the Arrhenius activation parameters.

2. Experimental

The synthesis of ylide·BH_3 (**2**), ylide·BPh_3 (**3**), ylide·$B(C_6F_5)_3$ (**4**), and ylide·BF_3 (**5**) as air-stable, crystalline complexes was previously described [2]. DSC curves were recorded on a DuPont 910 DSC instrument with Al_2O_3 as an internal reference standard with crimped aluminum pans (TA Instruments Part Nos. 900793.901 and 900794.901) under an atmosphere of N_2 (15 cm^3 s^{-1} flow rate). Sample masses between 8 and 10 mg of complexes **3**–**5** were used with a punched pinhole in the top of the pan for venting. Due to the extreme exothermicity of complex **2**, sample weights less than 1.5 mg and three punched pinholes in the sample pan were necessary to mitigate violent decomposition [5]. Scans between 25 and 400 °C were obtained at scan rates of 10, 7.5, 5.0, and 2.5 °C min^{-1} for complexes **3**–**5** and 5.0, 2.5, 2.0, 1.5, and 1.0 °C min^{-1} for complex **2** and a data collection rate of 10 point s^{-1}.

2.1. Computational methods

The ylide·$B(C_6F_5)_3$ and ylide·BPh_3 ground-state complexes were optimized at HF/3-21G(d) and HF/6-31G(d) using the GAUSSIAN-98 software package [6]. Transition state calculations were carried out by optimizing the structures with a constrained C_1–C_2 bond at 2.2 Å and C_2–S bond 2.5 Å with HF/3-21G(d). This starting geometry was used to locate the transition states by optimizing at HF/3-21G(d) and HF/6-31G(d) without constraints.

3. Results

An overlay of the DSC scans for complexes **2**–**5** at a heating rate of 10 °C min^{-1} is shown in Fig. 1. All scans show exothermic peaks. It was independently established that the products from complexes **2**–**4** are homologated organoboranes and dimethylsulfoxide. The rearrangement products of complex **5** that would occur from 1,2-fluorine migration could not be established. The exothermic reaction has been assigned to the 1,2-migration that occurs in the solid state for complexes **2**–**4**. It is straightforward to obtain kinetic data from DSC analyses with different heating rates. However, applying an appropriate model to obtain meaningful activation energies of solid-state reactions is more difficult [7]. Although the intent of this investigation is to obtain the relative migratory aptitudes and activation energies for the 1,2-migration step for complexes **2**–**4**, Arrhenius activation energies determined in the solid state do not correlate with those determined in homogeneous solution (or the gas phase). For example, induction delay, autocatalysis, and topochemical behavior is observed that may correspond to various modes of nuclei formation and rate acceleration [8,9]. More importantly, organic solids are often preceded or accompanied by melting upon reaction and two different rates of reaction, one from the melt, and one from the solid may complicate the kinetic analysis [10]. The following equation can be used to describe the kinetics of decomposition for both solid-phase and liquid-phase reactions:

$$\frac{d\alpha}{dt} = A \exp\left(-\frac{E}{R}\right) f(\alpha) \quad (1)$$

where α is the degree of conversion, $f(\alpha)$ is the kinetic expression that depends on the reaction model [9], E

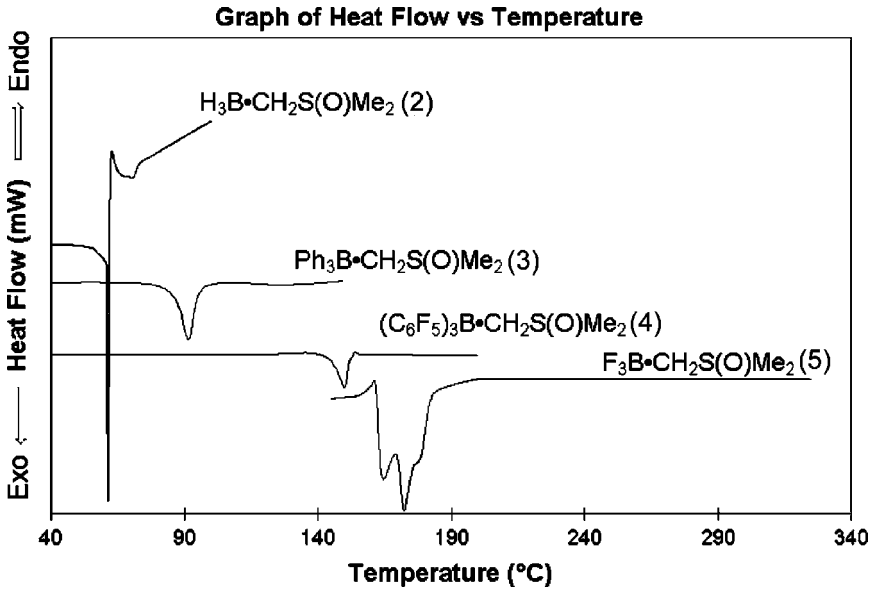

Fig. 1. DSC traces of ylide-borane complexes at 10 °C min^{-1} and arbitrary *y*-offset.

the apparent activation energy (J mol^{-1}), R the gas constant (J mol^{-1} K^{-1}), and A the Arrhenius frequency factor (time^{-1}).

Diffusion models (D_1, D_2, D_3), order of reaction models (F_1, F_2), geometrical models (R_2, R_3), and random nucleation models ($A_{1.5}$, A_2, A_3) were all considered as $f(\alpha)$ for complexes **2**–**5**. The kinetic model function $g(\alpha)$ and the relationship to temperature is expressed in a form that enables a master curve to be generated from a plot of all the non-isothermal data. In order to find the model that best-fits the experimental data, we applied the isoconversional integral method developed by Flynn and Wall [11] and Ozawa [12,13] with the Doyle approximation [14,15] in the form:

$$\log g(\alpha)\beta = \left[\log\left(\frac{AE}{R}\right) - 2.315\right] - 0.4567\frac{E}{RT} \quad (2)$$

where

$$g(\alpha) = \int_0^\alpha \frac{d\alpha}{f(a)} \quad (3)$$

where β is the heating rate (°C min^{-1}) and T the absolute temperature (K). This method is referred to as the Doyle equation throughout this paper. For each ylide-borane complex, a graph of $\log g(\alpha)\beta$ versus *1/T* was constructed over $0.1 < \alpha < 0.95$ for the composite DSC scans of all heating rates. The degree of conversion α was obtained from the DSC trace by integration of the partial peak area at different times. A linear plot with a high correlation coefficient (r) is used as the criterion to find the best model for the decomposition kinetics.

The plots of $\log g(\alpha)\beta$ versus $1/T$ for ylide·BF_3 (**5**) and ylide·BH_3 (**2**) complexes exhibited nonlinearity with every model tested. The ylide·BF_3 (**5**) complex exhibits multiple, exothermic peaks characteristic of multiple transformations. The accurate integration of these overlapping peaks was not possible. The peak width for the ylide·BH_3 (**2**) complex is narrow (30–60 s), even at heating rates of 1.0 °C min^{-1}. Since the data are obtained at a rate of 10 points min^{-1}, the peak is described by 5–10 data points. In addition, there is an ill-defined baseline for this complex as well (Fig. 1). These two factors led to inaccurate integration of the exothermic peak. Furthermore, upon reaction, significant amounts of gaseous reaction products are produced that oftentimes propelled the sample pan off the instrument's metal contacts. At scan rates of 10 °C min^{-1}, an audible pop was heard that corresponded with the separation of the two crimped sample pans, despite the presence of a large vent hole [5].

Heating a small amount of ylide·BH_3 (**2**) in an open micro-capillary to the onset of decomposition, for example, emits a green flash as pyrophoric gases, presumably methylborane, ignite in air while solid sample is thrusted halfway up inside the capillary. A clear, colorless, oily residue, presumably dimethylsulfoxide, is left behind along the length of the capillary. The DSC accessories required for gas-evolving samples were not available to us at the time and we opted not to pursue optimizing the data acquisition of this complex due to its rapid and very exothermic ($\Delta H = -230$ kJ mol^{-1}) reaction upon heating.

The data for the kinetic reactions of ylide·BPh_3 (**3**) and ylide·$B(C_6F_5)_3$ (**4**) complexes generated a number of linear plots and these two complexes will be discussed in detail. The fraction remaining $(1 - \alpha)$ is easily obtained from the integration of the DSC peak areas. The total heat released (H_{rxn}) from the exothermic 1,2-migration and the partial heat released at a particular time (H_t) are related to α, since $\alpha = H_t/H_{rxn}$. The graphs of fraction remaining $(1 - \alpha)$ versus temperature (°C) for ylide·BPh_3 (**3**) and ylide·$B(C_6F_5)_3$ (**4**) complexes are shown in Fig. 2. These values of α and T were used with Eq. (2) with each kinetic model [9] and a regression line was obtained for the composite data at all β.

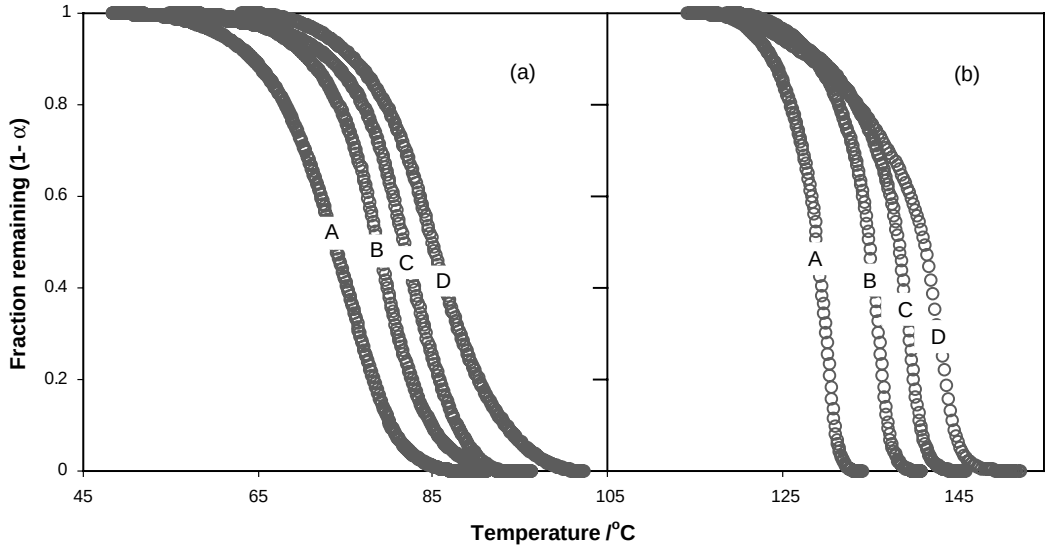

Fig. 2. Non-isothermal plots of fraction remaining $(1-\alpha)$ vs. temperature (°C) for (a) ylide·BPh_3 (**3**) and (b) ylide·$B(C_6F_5)_3$ (**4**). Heating rate—curve (A): 2.5 °C min^{-1}; curve (B): 5.0 °C min^{-1}; curve (C): 7.5 °C min^{-1}; curve (D): 10 °C min^{-1}.

Table 1
Models and kinetic parameters for ylide·BPh_3 (**3**) and ylide·$B(C_6F_5)_3$ (**4**)

Complex	Model	E_a (kJ mol^{-1})	A (min^{-1})	R
Ylide·BPh_3 (**3**)	$A_{1.5}$	120 ± 1	5.60 × 10^{17} (±0.8%)	0.9944
	A_2	93 ± 4	4.79 × 10^{13} (±4.0%)	0.9929
Ylide·$B(C_6F_5)_3$ (**4**)	R_2	248 ± 7	3.33 × 10^{30} (± 2.0%)	0.9693
	R_3	248 ± 5	1.64 × 10^{31} (±2.0%)	0.9691
	F_1	280 ± 5	1.00 × 10^{35} (±2.1%)	0.9664

The correlation coefficient (r) and the E_a and A values obtained from the equation of the best-fit lines are summarized in Table 1. Fig. 3 shows a plot of the E_a values at various α values for ylide·BPh_3 (**3**) and ylide·$B(C_6F_5)_3$ (**4**) complexes. The E_a for these complexes is fairly constant over the range of α used in the kinetic analyses, as expected [16].

The regression lines for R_2 and R_3 models fit well with the composite DSC data (Fig. 4) and F_1 (not shown) with ylide·$B(C_6F_5)_3$ (**4**) complex using scan rates of 5.0, 7.5, and 10 °C min^{-1}. The 2.5 °C min^{-1} set deviated significantly

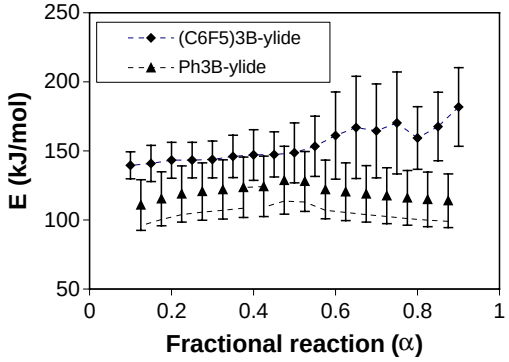

Fig. 3. Plots of the activation energy vs. α as estimated by the Ozawa method [12,13].

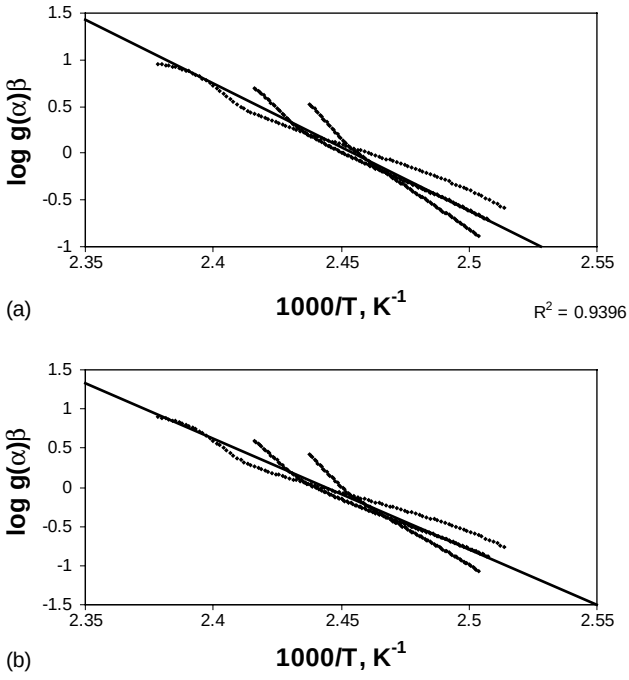

Fig. 4. Regression lines for the composite DSC data for ylide·$B(C_6F_5)_3$ (**4**) model: (a) R_2; (b) R_3.

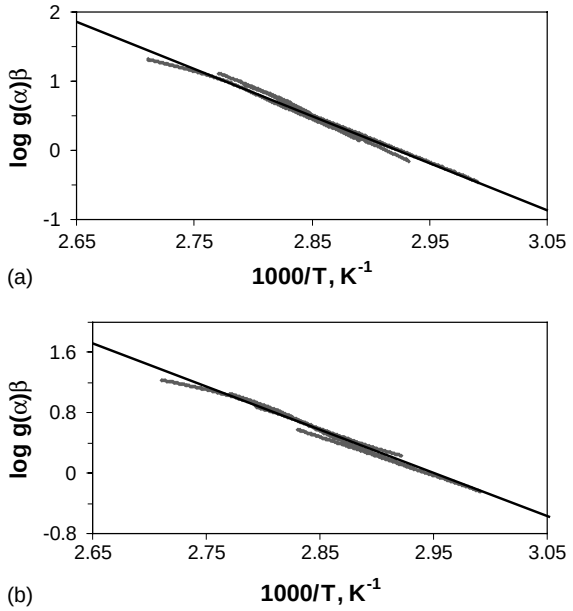

Fig. 5. Regression lines for the composite DSC data for ylide·BPh_3 model: (a) $A_{1.5}$; (b) A_2.

from the other data and was not included in the analysis since it was rejected with the *Q*-test (90% confidence limit). The slope and intercept of the regression line were used to calculate the Arrhenius activation parameters, which are listed in Table 1.

The regression lines for the $A_{1.5}$ and A_2 models fit well with the composite DSC data for ylide·BPh_3 (**3**) complex using scan rates of 2.5, 5.0, 7.5, and 10 °C min^{-1} (Fig. 5). In this case, the good data nearly coincide and it is difficult to identify individual heating curves from the composite overlay (Fig. 5). The derived Arrhenius activation parameters from these kinetic models are listed in Table 1. The calculated activation energies for the reaction of ylide·$B(C_6F_5)_3$ were similar for models R_2, R_3, and F_1. The calculated activation energies for the reaction of ylide·BPh_3 were similar for $A_{1.5}$ and A_2. It is common for the derived Arrhenius activation parameters to be similar for different kinetic models in solid-state reactions [9].

Table 2
Activation parameters for the 1,2-migration of ylide·borane complexes

	Ylide·$B(C_6F_5)_3$ (**4**)	Ylide·BPh_3 (**3**)
E_a (kJ mol^{-1})[a]	171 (±7)	129 (±8)
A (min^{-1})[b]	4.68×10^{21} (±4.5%)	1.04×10^{19} (±7.0%)
$\Delta H^{\ddagger}$ (kJ mol^{-1})[c]	168 (±7)	127 (±8)
$\Delta S^{\ddagger}$ (J mol^{-1} K^{-1})[d,f]	127 (±17)	76.6 (±12)
$\Delta G^{\ddagger}$ (kJ mol^{-1})[e,f]	130 (±1.7)	104 (±1.2)

[a] Eq. (4).
[b] Eq. (5).
[c] $\Delta H^{\ddagger} = E_a - RT$.
[d] $\Delta S^{\ddagger} = R \ln(Ah/ekT)$.
[e] $\Delta G^{\ddagger} = \Delta H^{\ddagger} - T\,\Delta S^{\ddagger}$.
[f] $T = 298$ K.

The exothermic peaks were often preceded by a falling baseline, and establishing the limits for integration was sometimes ambiguous. As a result there may be errors associated with the integration of peak areas, which are used to obtain α. In order to test the validity of previous calculations (Table 1), the method of Kissinger [17] was used, which does not require the extraction of α from the area under the DSC peaks. By studying the shift in the peak maximum T_m at different heating rates β the energy of activation E_a may be obtained by using Eq. (4). The Kissinger method uses only the peak maxima and does not rely on accurate integration of the peak areas to obtain α. The Arrhenius frequency parameter A was obtained using Eq. (5) [17].

$$\frac{d(\ln(\beta/T_m^2))}{d(1/T_m)} = -\frac{E_a}{R} \tag{4}$$

$$A = \beta \frac{E_a}{RT_m^2} e^{E_a/RT} \tag{5}$$

The plots of $\ln(\beta/T_m^2)$ versus $1/T_m$ for the reaction of ylide·BPh_3 (**3**) and ylide·$B(C_6F_5)_3$ (**4**) complexes are shown in Fig. 6 and yield the kinetic parameters, which are listed in Table 2.

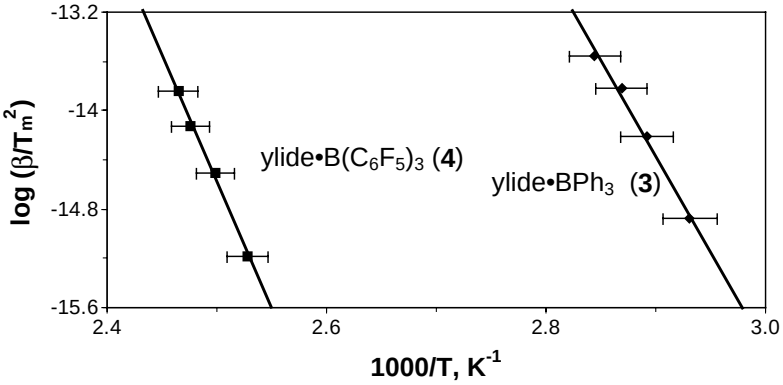

Fig. 6. Plots of $\ln(\beta/T_m^2)$ vs. $1/T_m$ for the reaction of ylide·BPh_3 (**3**) and ylide·$B(C_6F_5)_3$ (**4**).

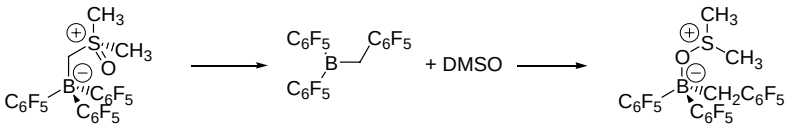

Scheme 2. Reaction of ylide·$B(C_6F_5)_3$ (**4**) produces a DMSO organoborane complex.

4. Discussion

The conversion plots of ylide·$B(C_6F_5)_3$ (**4**) and ylide·BPh_3 (**3**) (Fig. 2) differ in shape and may indicate differences in models of topochemical reaction or other complications. For example, the 1,2-migration of ylide·$B(C_6F_5)_3$ (**4**) produces a strong Lewis acid and DMSO, which are capable of combining to form an organoborane·DMSO complex (Scheme 2) [2]. This complexation is expected to be exothermic and will cause the conversion plots to be inaccurate due to errors in integration. However, the activation energies obtained using the model-free Flynn–Wall–Ozawa method [12,13] (Fig. 3) are constant over the α considered and establish a basis for using the data in subsequent kinetic analyses [18,19].

The kinetic analysis of the decomposition of ylide·BPh_3 (**3**) with the Kissinger method ($E_a = 129\,kJ\,mol^{-1}$, $A = 1.04 \times 10^{19}\,min^{-1}$) and Doyle's equation using the $A_{1.5}$ model ($E_a = 120\,kJ\,mol^{-1}$, $A = 5.60 \times 10^{17}\,min^{-1}$) gave consistent results for calculated values of both E_a and A. The satisfactory agreement between these data demonstrates that obtaining rates of initiation is amenable by this DSC methodology.

The kinetic analysis of the decomposition of ylide·$B(C_6F_5)_3$ (**4**) with the Kissinger method ($E_a = 171\,kJ\,mol^{-1}$, $A = 4.68 \times 10^{21}\,min^{-1}$) and Doyle's equation using the R_2, R_3, and F_1 models ($E_a = 248$–$280\,kJ\,mol^{-1}$, $A = 3.33 \times 10^{30}$to$1.00 \times 10^{35}\,min^{-1}$) deviated significantly. It is believed that the conversion plots used for Doyle's equation contain significant error due to the exothermicity associated with complexation of DMSO to the homologated organoborane $(C_6F_5)_2BCH_2(C_6F_5)$ (Scheme 2). The activation parameters obtained with the Kissinger method may not be affected as much, due to the exothermic complexation, since α and peak areas are not determined using this method.

The energy of activation for the reaction of ylide·BPh_3 (**3**) and ylide·$B(C_6F_5)_3$ (**4**) are consistent with a solid that undergoes transition upon heating above room temperature ($E_a > 105\,kJ\,mol^{-1}$) [2]. The gas-phase ab initio HF/6-31G(d) calculations of activation energies for ylide·Ph_3B ($E_a = 67\,kJ\,mol^{-1}$) and ylide·$B(C_6F_5)_3$ ($E_a = 92\,kJ\,mol^{-1}$) parallel the relative reactivity of the experimentally derived energies of activation (see Fig. 7). The entropies of activation ($\Delta S^{\ddagger} > 0$) are consistent with a unimolecular decomposition to two fragments [20]. The Kissinger method was used to obtain the entropies of activation for ylide·BPh_3 (**3**) ($\Delta S^{\ddagger} = 76.6 \pm 12\,J\,mol^{-1}\,K^{-1}$) and ylide·$B(C_6F_5)_3$ (**4**) ($\Delta S^{\ddagger} = 127 \pm 17\,J\,mol^{-1}\,K^{-1}$). Due to lengthy computational times, the frequency calculations for ylide·$B(C_6F_5)_3$ (**4**) and ylide·BPh_3 (**3**) transition states were not performed at HF/6-31G(d) to obtain the entropies directly. However, the transition state for ylide·$B(C_6F_5)_3$ (**4**) exhibits both a shorter C_1–C_2 bond (2.240 Å) and C_2–S bond (2.400 Å) than the ylide·BPh_3 (**3**) transition state (C_1–$C_2 = 2.250$ Å, C_2–S = 2.453 Å). This suggests that the transition state for ylide·$B(C_6F_5)_3$ (**4**) is more ordered compared with ylide·BPh_3 (**3**). In solution the ylide·BPh_3 complex undergoes phenyl 1,2-migration at 23 °C while the ylide·$B(C_6F_5)_3$ complex is unreactive at 23 °C, these differences also parallel the trends in the solid state.

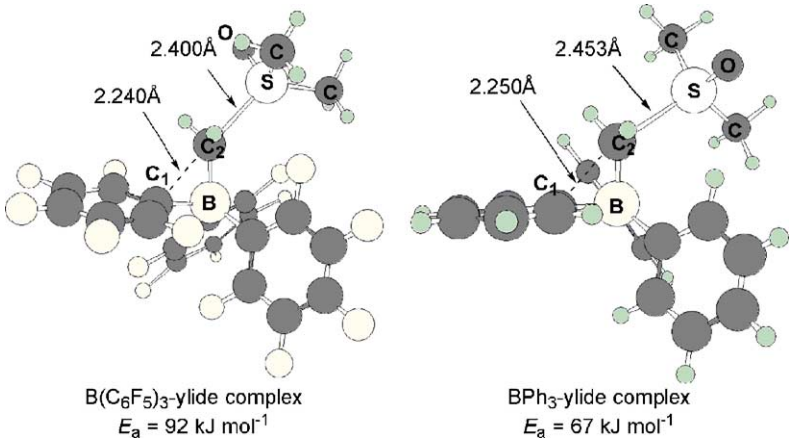

Fig. 7. HF/6-31G(d) calculated transition-state structures for ylide·BPh_3 (**3**) and ylide·$B(C_6F_5)_3$ (**4**).

5. Conclusion

The Arrhenius activation parameters for the reaction of ylide·Ph_3B (**3**) and ylide·$B(C_6F_5)_3$ (**4**) were obtained using Doyle's equation and Kissinger's method. The kinetics of 1,2-migration best-fit with R_2, F_3, F_1 models for ylide·Ph_3B (**3**), and $A_{1.5}$ and A_2 models for ylide·$B(C_6F_5)_3$ (**4**). The two methods provided similar kinetic parameters with an activation energy for the reaction of ylide·$B(C_6F_5)_3$ (**4**) greater than for the reaction of ylide·Ph_3B (**3**). HF/6-31G(d) calculations substantiate the finding that C_6F_5 1,2-migration in complex **4** had a higher E_a and $\Delta S^{\ddagger}$ than C_6H_5 1,2-migration in complex **3**.

Acknowledgements

This research was supported from a grant from the National Sciences Foundation (CHE-9617475).

References

[1] K.J. Shea, B.B. Busch, M.M. Paz, C.L. Staiger, J.M. Stoddard, J.R. Walker, X. Zhou, H. Zhu, J. Am. Chem. Soc. 124 (2002) 3636.
[2] J.M. Stoddard, K.J. Shea, Organometallics 22 (2003) 1124.
[3] S. Vyazovkin, Int. Rev. Phys. Chem. 19 (2000) 45.
[4] J.D. Sewry, M.E. Brown, Thermochim. Acta 390 (2002) 217.
[5] Caution, the BH_3-ylide complex has been prepared in 3 g quantities as a white solid substance. The DSC (<1.5 mg) shows a very exothermic transition above 55 °C and larger amounts of solid complex should not be heated.
[6] M.J. Frisch, et al., GAUSSIAN 98, Revision A.11, Gaussian, Inc., Pittsburgh, PA, 2001.
[7] A.K. Galwey, Thermochim. Acta 399 (2003) 1.
[8] E. Davydov, A. Vorotnikov, G. Pariyskii, G. Zalkov, Kinetic Peculiarities of Solid Phase Reactions, John Wiley & Sons, New York, 1998.
[9] A.K. Galwey, M.E. Brown, Thermal Decomposition of Ionic Solids, Elsevier, Amsterdam, 1999.
[10] C.E. Bawn, Chem. Solid State (1955) 254.
[11] J.H. Flynn, J. Wall, Nat. Bur. Stand. 70A (1966) 487.
[12] T. Ozawa, Bull. Chem. Soc. Jpn. 38 (1965) 1881.
[13] T. Ozawa, J. Therm. Anal. 2 (1970) 301.
[14] D. Doyle, J. Appl. Polym. Sci. 5 (1961) 285.
[15] B. Budrugeac, D. Homentcouschi, E. Segal, J. Therm. Anal. Cal. 63 (2001) 457.
[16] S. Vyazovkin, New J. Chem. 24 (2000) 913.
[17] H. Kissinger, J. Res. Nat. Bureau Standards 57 (1956) 217.
[18] S. Vyazovkin, C.A. Wright, Thermochim. Acta 340/341 (1999) 53.
[19] S.V. Vyazovkin, J. Comput. Chem. 22 (2001) 178.
[20] T.H. Lowry, K.S. Richardson, Mechanism and Theory in Organic Chemistry, 2nd ed., Harper & Row, New York, 1981.